

Comparison of the MPPT command based on the PSO, P&O, and IncCond algorithm implemented in Dspace

GHITA BENNIS

LIMAS Laboratory
Faculty of Sciences Dhar El
Mahraz
Sidi Mohammed Ben
Abdellah University
FEZ, MOROCCO

KARIM MOHAMMED

LIMAS Laboratory
Faculty of Sciences Dhar El
Mahraz
Sidi Mohammed Ben
Abdellah University
FEZ, MOROCCO

AHMED LAGRIOUI

Department of Electrical
Engineering and Computer
Engineering
National School of Arts and
Métiers
National School of Arts and
Métiers
Meknes, MOROCCO

Abstract: Several algorithms have been offered to track the maximum power point when we have one maximum power point. In this paper, we will propose an improved maximum power point tracking method for the photovoltaic system that utilizes a modified PSO algorithm. The main advantage of the method is the decreasing of the steady-state oscillation (to practically zero) once the maximum power point is located. moreover, the proposed method has the ability to track the maximum power point under extreme environmental conditions. To evaluate the effectiveness of the proposed method, MATLAB simulations are carried out under very challenging circumstances, namely step changes in irradiance and step changes in load. Finally, its performance is compared with the «perturbation and observation» and incremental conductance.

The results obtained were validated by a PIL (Processor In the Loop) co-simulation using the DSpace 1104 card.

Keywords: PSO, P&O, MPPT, BOOST, INCREMENTAL CONDUCTANCE, Dspace1104

Received: February 13, 2023. Revised: November 6, 2023. Accepted: December 7, 2023. Published: January 16, 2024.

1. Introduction

In a photovoltaic system, light energy can be directly converted into electrical energy. [1, 2] And this is through the use of sensors made of semiconductor materials sensitive to the wavelengths of the visible, which are called "photovoltaic" cells "PV". We call a photovoltaic generator. (GPV) the association of several PV cells in series and / or parallel, The photovoltaic generator is essentially distinguished by its static current-voltage characteristic $I(V)$ which is nonlinear in nature and which has a maximum power point (PPM). This characteristic has a direct relation with the level of illumination, the temperature of the cell, and the aging of the whole. In fact, determining the operating point of the GPV depends directly on the load to which it is connected. This operating point is more or less distant from the PPM which is characterized by the most optimal current and voltage. For the conversion of photovoltaic energy in terms of efficiency to be optimized, a PPM tracking mechanism called "Maximum Power Point Tracking" (MPPT) is necessary to ensure the generation of maximum power. In the literature, there are several methods divided into conventional methods (perturbation and Observation ...) and innovative methods (optimization of particle swarms)[6-8].

2. Principle of Maximum Point Search (MPPT)

An MPPT (Maximum Power Point Tracker) is a command which is associated with an adaptation stage (DC-DC converter) and which allows the photovoltaic generator to maintain the production, permanently, of the maximum of its power. The role of the control technique is to control the static converter that connects the load, it makes it possible to act on the duty cycle automatically to bring the generator to its optimal operating value despite meteorological instabilities or even sudden fluctuations charges occurring from time to time[3-5].

2.1 Perturbation & observation (P&O) method

Figure 1 shows the variation of power as a function of the voltage of a photovoltaic panel. It can be seen that, if a voltage disturbance occurs, the photovoltaic power increases and the direction of disturbance is maintained. Otherwise, it is reversed in order to resume convergence to a new PPM. The trajectory of the variation of these points is shown in Figure 1.

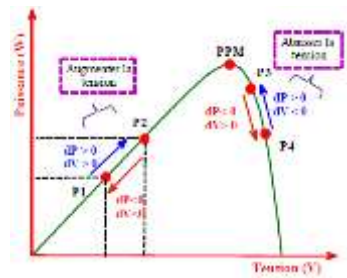


Fig. 1. Power available depending on the voltage across the PV generator

2.2 MPPT based on the conductance increment

The PPM can be reached by comparing the value of the conductance (I_{pv}/V_{pv}) with that of the increment of conductance (dI_{pv}/dV_{pv}) at all times. Figure 3 shows the algorithm of this method, where V_r represents the reference voltage [9].

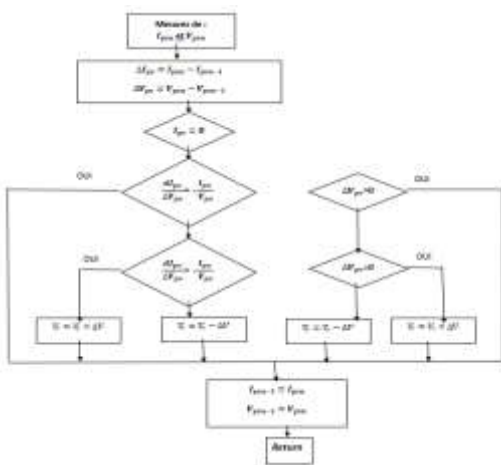
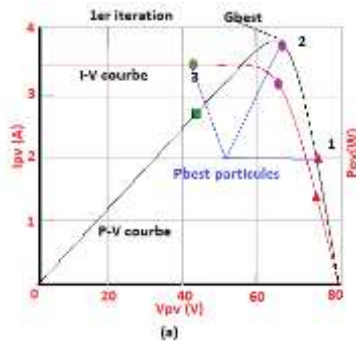
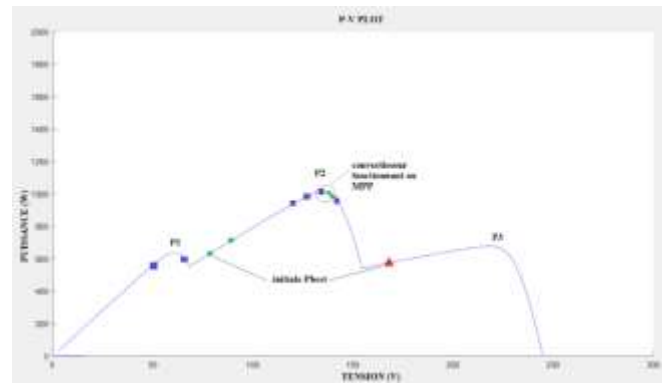
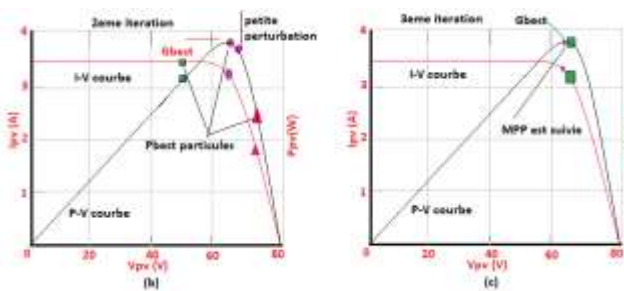


Fig. 2. Algorithm of the conductance increment method.

2.3 MPPT based on the PSO



A. one peak



B. Multiple peaks (partial shading)
 Fig. 3. PSO particle movements in MPP research

To start the optimization process, the algorithm can transmit up to three operating cycles d_i ($i = 1, 2, 3$) to the power converter. In Figure 4, the work cycles d_1 , d_2 , and d_3 are mentioned by triangular, circular, and square points, respectively. These duty cycles play the role of P_{best} at the level of the first iteration. Of these, d_2 is the G_{best} that provides the best fitness value (which is the power of the array), as shown in Figure 4 (a). At the second iteration, the resulting speed is only due 'at the term G_{best} . The factor $(P_{best} - d_i)$ is zero. In addition, the G_{best} speed of the particle (d_2) is equal to zero also since $(G_{best} - d_2)$ is zero. This results in zero speed and, therefore, the duty cycle remains invariable. Hence, this particle will not contribute to the exploration process. To avoid such a problem, a small disturbance of the duty cycle is introduced, since it is well authorized, as shown in Figure 4 (b), to ensure the modification of the value of the physical condition. Fig. 4 (c) mentions the movement of particles at the level of the third iteration. As all the work cycles in the previous iteration lead to a better aptitude value, the direction of the speed of these particles remains unchanged, and thereafter they move towards G_{best} in the same direction. In the third iteration, all operating cycles (d_i , $i = 1, 2, 3$) reach the MPP with a low velocity value. In the following iteration, because of the very low speed, the value of the duty cycle approaches a constant. Hence, the operating point will be maintained and the oscillation around the MPP will be minimized[10-13].

2.4 MPPT based on the PSO multiple pics

When the PV array operates under uniform solar insolation, the resulting P-V characteristic curve of the array exhibits a single MPP. However, under partial shading, the P-V curves are characterized by multiple peaks, i.e. with several local peaks and one global peak, as shown in Fig. 3.B. In this example, the i-V curve is characterized by three peaks, while the p-V curve is characterized by three peaks. These are labeled P1, P2, P3. It can be observed that the time derivative of the power dP/dV is zero for the global peaks and for all local peaks. In addition, the slope on its right and left sides has the same signs. Since all conventional MPPT methods are based on the slope and sign value of dP/dV , the algorithm could not properly distinguish the local peaks

(P1, P2, and P3) and the global peak (P2). It is very likely that MPPT is forced to trap in the local peak, leading to a reduction in power output and thus significantly deteriorating the efficiency of the PV system [13].

However, since the PSO method works based on the basis of the research technique, the overall peak can be tracked without difficulty. Figure 3.B illustrates the tracking capability of PSO during partial shading. Similarly to the previous P-V curve, the proposed method conveys three duty cycles, which serve as Pbest particles. It can be seen that the voltage and current that contribute to these initial duty cycles (Pbesti) are far from the overall peak (P2). But in later stages of iterations, it has successfully found the global vertex P2.

3. Simulation of Search for the Maximum Point of Power

Different tracking algorithms have been proven and used with several types of DC-DC. Among these algorithms, we studied here the methods "Perturb and observ" "and" conductance increment "and" PSO ". The choice of converter is a preliminary step in having a more efficient MPPT control. The boost-type DC-DC converter allows the photovoltaic system to follow the PPM at all times, independently of temperature, sunshine and load.

The photovoltaic system consists of a photovoltaic panel, a DC-DC converter of the boost type provided with its MPPT control, which is based on the P&O algorithm, and a pulse width modulation generator (PWM) in order to check the duty cycle of the converter for a resistive load. The synoptic diagram is mentioned in figure 5.

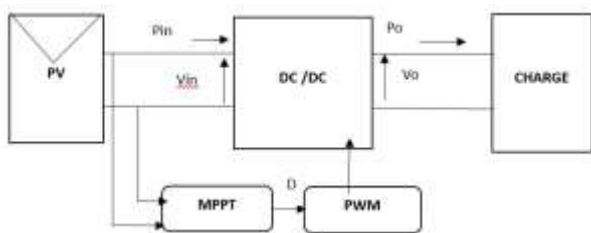


Fig. 4. Synoptic diagram of the system studied.

we have made the simulation with Matlab-Simulink of the curves of input and output voltages as well as those of input and output currents of the converter for a constant sunshine of 1000W / m2 and constant temperature of 25 ° C, and a resistive load. FIG. 5 illustrates the results of the simulation of the input and output values, and Fig. 6 clearly illustrates the input (Pin) and output (Po) power,

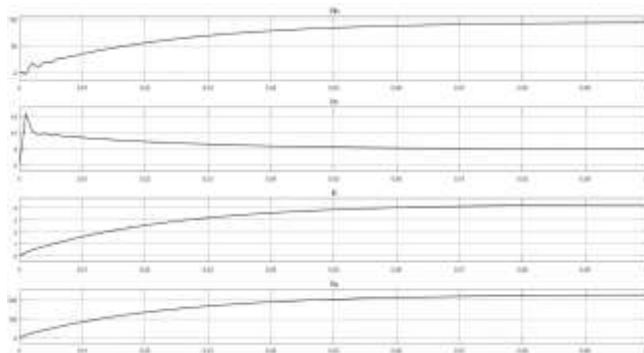


Fig. 5. Input voltage V_{in} , input current I_{in} , output current I_o , output voltage V_o

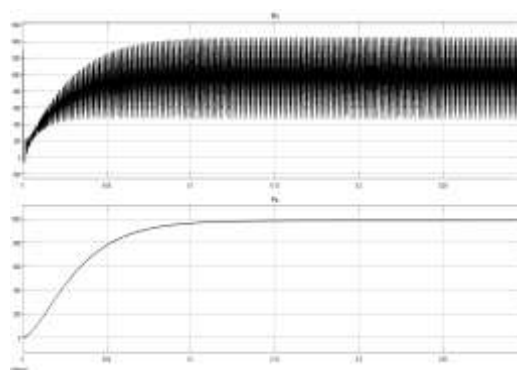


Fig. 6. P_{in} input power, P_o output power

In figures (6 and 7), and for a constant illumination of 1000 W / m2 and a temperature of 25 ° C, the typical results of simulation of the electrical characteristics at the output of the panel and at the output of a chopper of controlled elevator type by the MPPT command. It clearly appears that: The different electrical quantities (powers, voltages, and currents) are stable and unchanging. After a transient regime of duration 0.05 s, the MPPT command oscillates the operating point around the PPM point.

The power given by the PV generator reaches a stable value around 1200 W and that supplied to the load around 1000 W, at the output of the panel, the voltage and the current stabilize respectively around 100 V and 5 A.

At the level of the load, the voltage and the current stabilize respectively around 230 V and 4.5 A.

Note that the difference between the power output from the panel and that supplied to the load does not exceed 200 watts. These losses are attributed to the

different losses by switching and by conduction in the Mosfet transistor, in the diode, and in the various components of the MPPT control.

- Influence of lighting and temperature on the instantaneous evolution of V and P

The results of the simulation that have undergone variations in the illumination and the temperature are

mentioned in Figs. (8) to (11), we presented the power and input voltage of the converter as well as the power and the voltage of the converter output (across the load).

✓ Temperature Variation Case

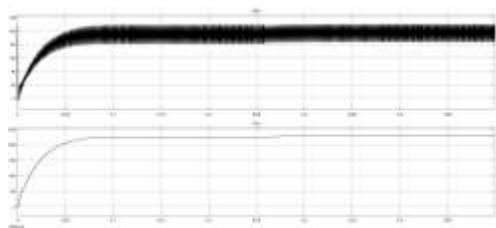


Fig. 7. Voltage generated by the PV panel (V_{in}), voltage across the load (V_o) for $1000W / m^2$ and variable temperature from $50^\circ C$ to $25^\circ C$.

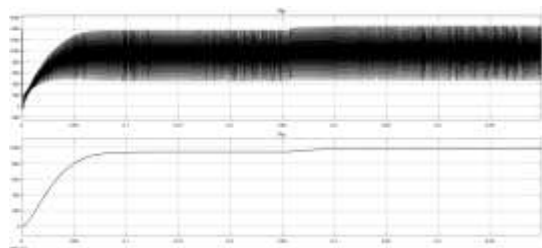


Fig. 8. The power generated by the PV panel (P_{in}) and the output power consumed by the load (P_o) for $G = 1000W / m^2$ and variable temperature from $50^\circ C$ to $25^\circ C$

Figure (8) shows the evolution of the voltage produced by the PV panel as well as across the load. Note that the voltage increases with decrease in temperature ($50^\circ C$ to $25^\circ C$). Figure (9) shows the evolution of the power generated by the PV panel and that consumed by the load.

✓ Case of the variation of the lighting

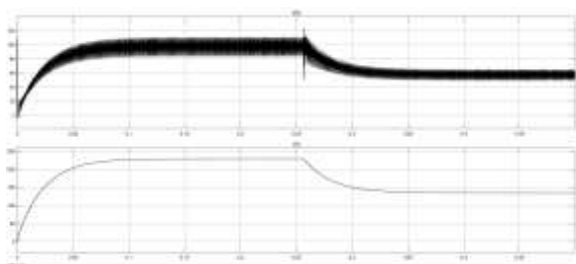


Fig. 9. Fig. 10. Voltage generated by the PV panel (V_{in}), voltage across the load (V_o) for $T = 25^\circ C$ and variable lighting from $G = 1000W / m^2$ to $750 W / m^2$

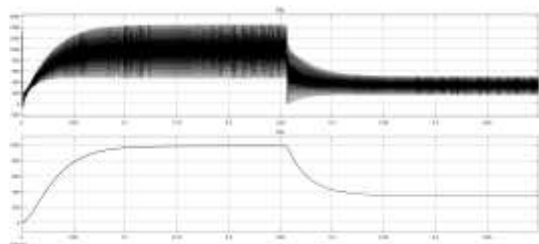


Fig. 10. The power generated by the PV panel (P_{in}) and the output power consumed by the load (P_o) for $T = 25^\circ C$ and variable lighting from $G = 1000W / m^2$ to $750 W / m^2$

Figure (11) shows the evolution of the power generated by the PV panel and that consumed by the load. It is noted that the power increases with increasing illumination from $750W / m^2$ to $1000W / m^2$. Figure (10) shows the evolution of the voltage generated by the PV panel and that across the load. It is noted that the voltage increases with the increase in the illumination from $750W / m^2$ to $1000W / m^2$.

3.1 MPPT control based on conductance increment

Figure 12 shows the Matlab / Simulink diagram of the INC-type MPPT command applied to the PV system.

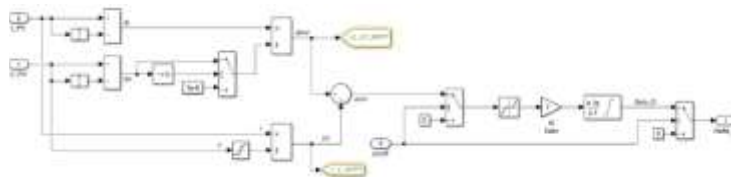


Fig. 11. Simulation diagram of the MPPT command (INC)

Figures (13) to (14) show the evolution of the voltage generated by the PV panel and that throughout the load for an illumination $G = 1000W / m^2$ and a temperature $T = 25^\circ C$.

Figures (15) to (16) show the evolution of the current generated by the PV panel and that at the terminals of the load for an illumination $G = 1000W / m^2$ and a temperature $T = 25^\circ C$.

Figures (17) to (18) show the evolution of the power generated by the PV panel and that consumed by the load for an illumination $G = 1000W / m^2$ and a temperature $T = 25^\circ C$.

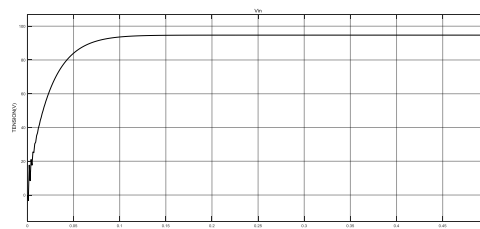


Fig. 12. the voltage generated by the PV panel for $G = 1000W / m^2$ and $T = 25^\circ C$.

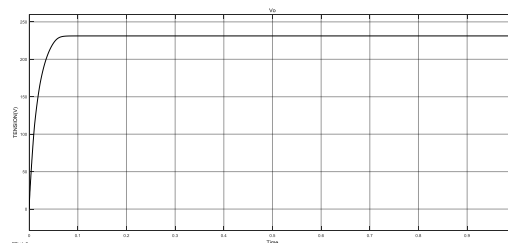


Fig. 13. the voltage consumed by the load $G = 1000W / m^2$ and $T = 25^\circ C$

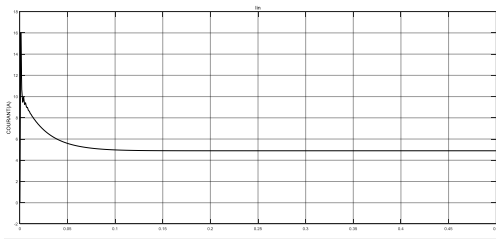


Fig. 14. the current generated by the PV panel for $G = 1000W / m^2$ and $T = 25^\circ C$

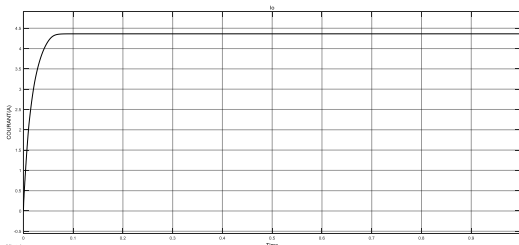


Fig. 15. The current consumed by the load $G = 1000W / m^2$ and $T = 25^\circ C$

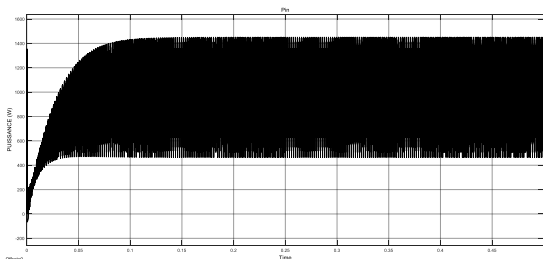


Fig. 16. the power generated by the PV panel for $G = 1000W / m^2$ and $T = 25^\circ C$.

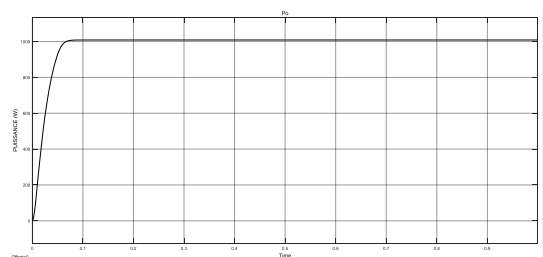


Fig. 17. Puissance consumed by the charge $G=1000W/m^2$ et $T=25^\circ C$

As a general remark concerning the evolution of the voltage and the power, although we started the simulation with zero initial conditions, the incremental MPPT command of conductance allowed us to obtain the nominal operating point of our load for illumination and a standard temperature. The different electrical quantities: powers, voltages, and currents are stable. After a transient state of 0.05 s, the MPPT command oscillates the operating point around the point of the PPM.

The power established by the PV generator reaches a stable value around 1200 W and that supplied to the load around 1010 W, at the output of the panel, the voltage and the current stabilize respectively around 100 V and 4.5A.

At the level of the load, the voltage and the current stabilize respectively around 230 V and 4.4 A.

It should be noted that the difference between the power output from the panel and that supplied to the load does not exceed 190 watts. These losses are attributed to the switching and conduction losses in the Mosfet transistor, in the diode, and in the various components of the MPPT control.

- Influence of lighting and temperature on the instantaneous evolution of V and P

The results of the simulation with variations of the illumination and the temperature are described by figures (19) to (26), where we mentioned the power and the input voltage of the converter as well as the power and output voltage of the converter (across the load).

✓ Temperature Variation Case

Figures (19) and (27) show the evolution of the voltage produced by the PV panel and that across the load. Note that the voltage increases with the decrease in temperature ($50^\circ C$ to $25^\circ C$). Figures (21) and (22) show the evolution of the power generated by the photovoltaic panel and that consumed by the load. We note that the power increases with decreasing temperature ($50^\circ C$ to $25^\circ C$).

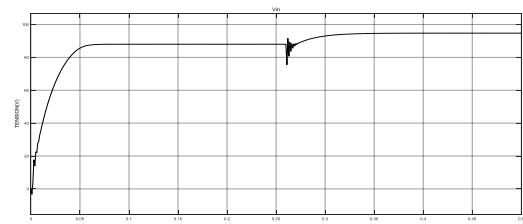


Fig. 18. Voltage generated by the PV panel with a temperature variation $50^\circ C$ to $25^\circ C$

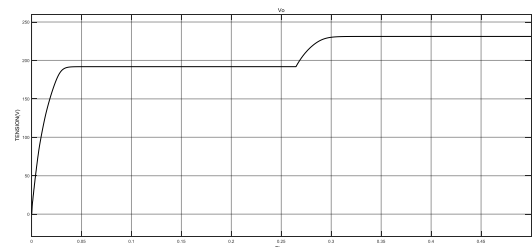


Fig. 19. Voltage across the load with a temperature variation from $50^\circ C$ to $25^\circ C$

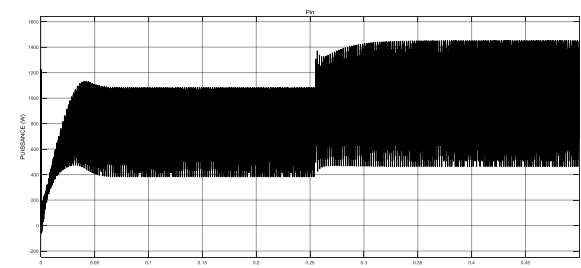


Fig. 20. Power generated by the PV panel with a temperature variation of $50^\circ C$ to $25^\circ C$

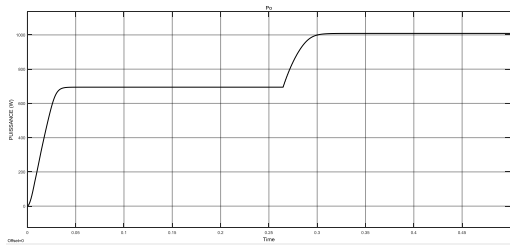


Fig. 21. Power at the load terminals with a temperature variation from 50 ° C to 25 ° C

✓ Case of variation of the lighting

Figures (23) and (24) show the evolution of the power generated by the PV panel and that consumed by the load. It is noted that the power increases with increasing illumination from 750W / m² to 1000W / m². Figures (25) and (26) show the evolution of the voltage generated by the PV panel and that across the load. It is noted that the voltage increases with the increase in the illumination from 750W / m² to 1000W / m².

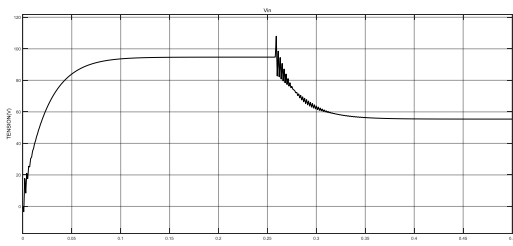


Fig. 22. Voltage generated by the PV panel for variable lighting 1000 W / m² to 750w / m²

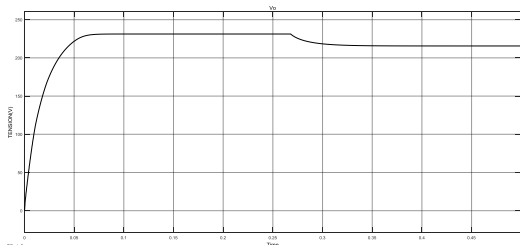


Fig. 23. Voltage across the load variable lighting 1000 W / m² to 750w / m²

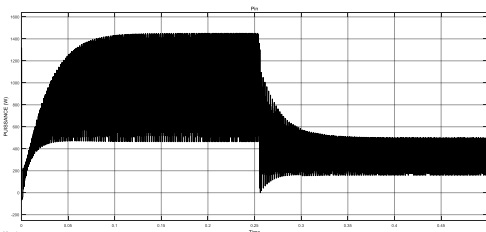


Fig. 24. Power generated by the PV panel for variable lighting from 1000W / m² to 750W / m²

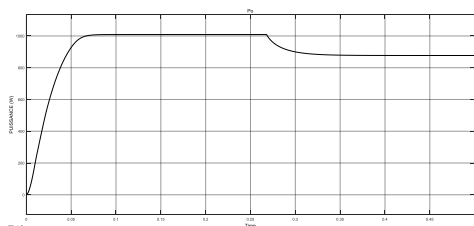


Fig. 25. Power across the load variable lighting 1000 W / m² to 750w / m²

3.2 MPPT control based on PSO

In this section we present the techniques for calculating the parameters of the PSO command, as well as the results of the MATLAB / Simulink simulation of the PV system used with the PSO type command.

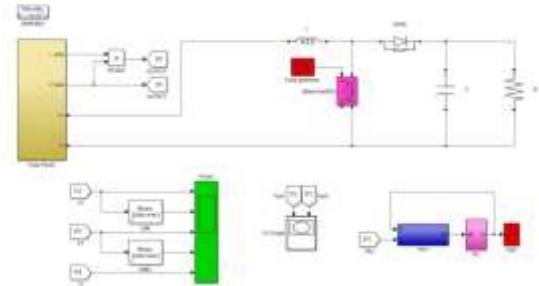


Fig. 26. Diagram of the complete PSO system

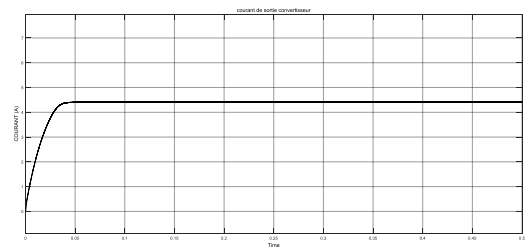


Fig. 27. The current consumed by the load for G = 1000W / m² and T = 25 ° C

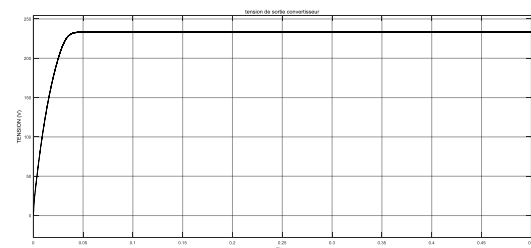


Fig. 28. the voltage consumed by the load for G = 1000W / m² and T = 25 ° C.

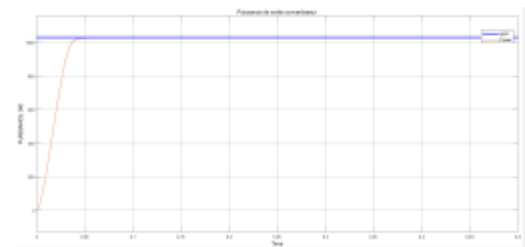


Fig. 29. the power consumed by the load for G = 1000W / m² and T = 25 ° C.

In the figures (28 to 30), and for a constant illumination of 1000 W / m² and a temperature of 25 ° C, the typical results of simulation of the electrical characteristics at the output of the panel and at the output of a chopper of controlled elevator type by the MPPT command clearly appears that: The different electrical quantities (powers, voltages, and currents) are stable. After a transient state of 0.03 s, the MPPT command

oscillates the operating point around the point of the PPM.

The power supplied by the PV generator reaches a stable value around 1200 W and that supplied to the load around 1030 W, at the output of the panel, the voltage and the current stabilize, respectively, around 100 V and 5 A.

At the level of the load, the voltage and the current stabilize respectively around 235 V and 4.5 A.

Note that the difference between the power output from the panel and that supplied to the load does not exceed 170 Watts. These losses are attributed to the switching and conduction losses in the Mosfet transistor, in the diode, and in the various components of the MPPT control.

3.3 Comparison of MPPT commands

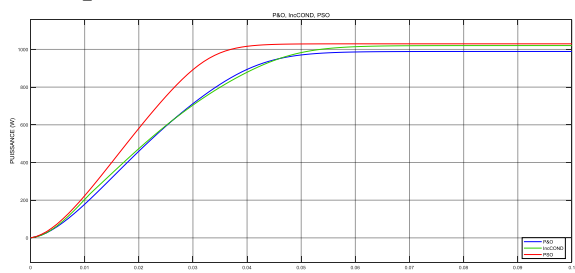


Fig. 30. PSO, P&O and IncCond train MPP monitoring

Figure 31 shows a comparison between the power extracted from the solar panel of PSO, P & O and incremental conductances. Based on the results in Figure 31, we can conclude that the PSO MPP gives high accuracy by comparing it to that of P & O and IncCond.

| | | BOOST converter output | | |
|------------------------------------|--|--|--|--------------------------------------|
| BOOST converter input | Algorithm P&O | Algorithm incCond | Algorithm PSO | |
| | | | One peak | multi peaks |
| Vin= 118W Iin= 9A Pin= 1062W | Pout= 1000W Vout= 230V Iout= 4,34A η= 94% | Pout= 1200W Vout= 230V Iout= 4,43A η= 96% | Pout= 1030W Vout= 233V Iout= 4,4 A η= 97% | Pout= 800W Vout= 160V Iout= 5A |

3.4 PSO Multiple peaks

The role of the PSO block is to direct the system to MPPG (maximum overall power) with a slight error, then stabilize the system to the maximum. Figure 3.31 shows the schematic of the complete system.

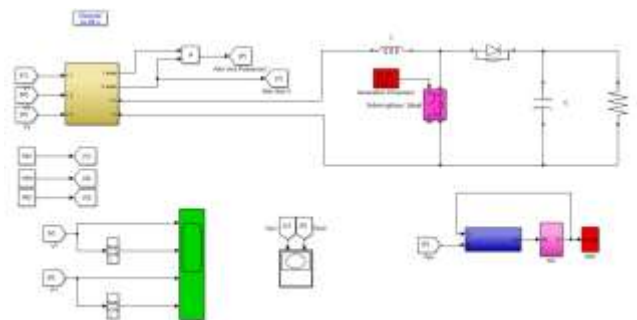


Fig. 31. Schematic of the complete multipeak PSO system

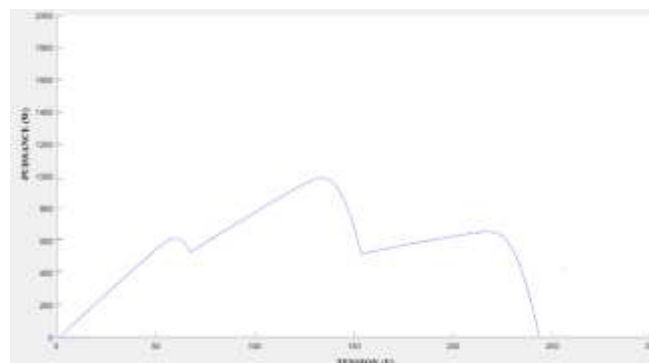


Fig. 32. shows the characteristic curve of the PV system under the following insolation: E1=500 W/m², E2=1000 W/m², E3 = 600 W/m².

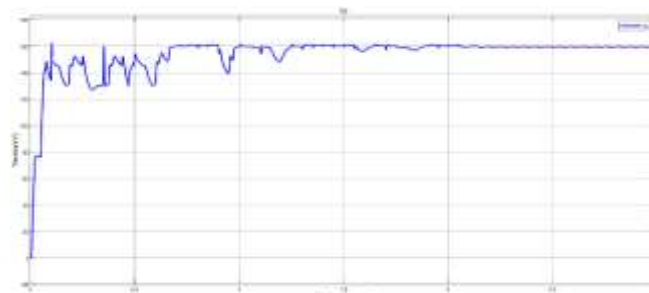


Fig. 33. BOOST converter output voltage

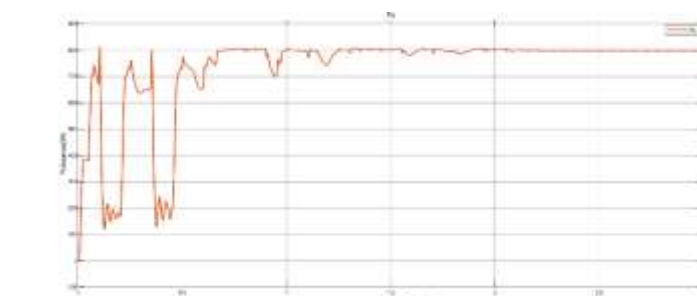


Fig. 34. BOOST converter output power

Due to non-uniform solar insolation, the resulting P-V characteristic curve of the SP exhibits multiple peaks, as shown in Figure 32. Figures 33, 34, respectively, show the voltage and power of the photovoltaic panel obtained using the PSO algorithm.

3.5 PIL simulation DSpace

In previous chapters, we used Simulink to model our system. With S-function and Stateflow techniques, complicated systems, and discrete event systems can be modeled and simulated. We also studied all the numerical simulation approaches in Simulink. However, interaction with the real world has not been considered until now. Simulink models cannot be built due to the complexity of real systems, the system must be integrated into the simulation loop to obtain more accurate simulation results; this type of simulation is usually called processor-in-the-simulation loop (PIL). The Workbench provided by MathWorks can translate Simulink models into C code, and standalone executable files can also be generated using this tool, so that control can be performed. Examples of these products are dSPACE, with its Control Desk and Quanser plus WinCon (which can be used to implement processor-in-the-loop simulation). MATLAB and Simulink support many products from well-known hardware manufacturers such as Motorola, Texas Instruments, etc., and can directly generate executable code for them from Simulink models. Network simulators or programmable DC power supply are expensive instruments and they are not always affordable. Therefore, PIL testing can be used as an inexpensive solution to test hardware implementation of the MPPT algorithm and inverter control command. As part of this work, we used a DSpace 1104 card with its control desk to implement the processor-in-the-loop simulation. In the following, we will present the different results obtained by the PIL simulation for the MPPT command.

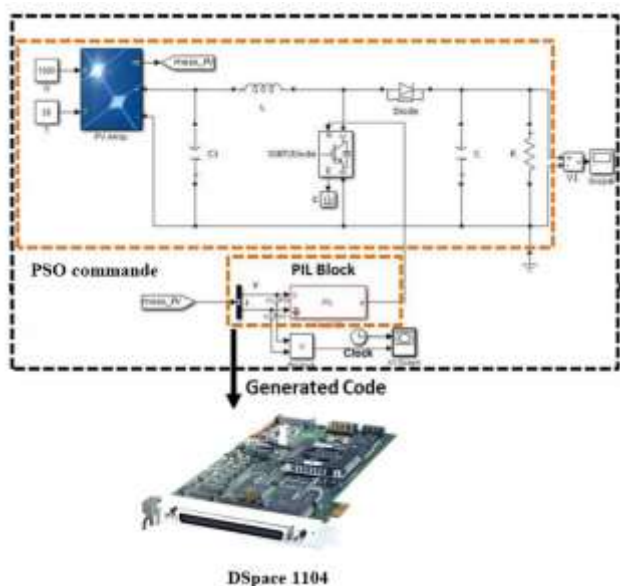


Fig. 35. PV system using the PIL block.

Figure 35 represents the simulation / cosimulation diagram of the first part of our system composed of a PV generator, a boost converter, an MPPT control based on PSO control and a resistive load, we let's carry out the co-simulation for $E1 = 300$, $E2=700$ and $E3=1000$ W/m².

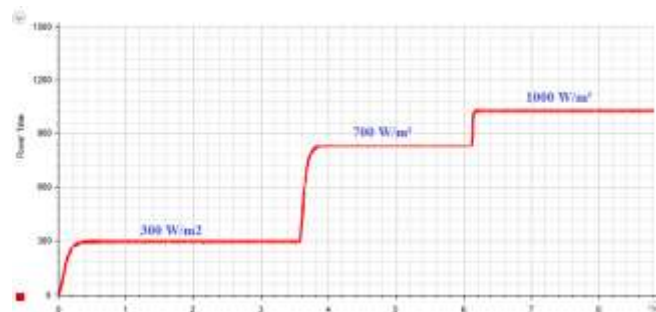


Fig. 36. the power at the output of the boost converter (Pout);

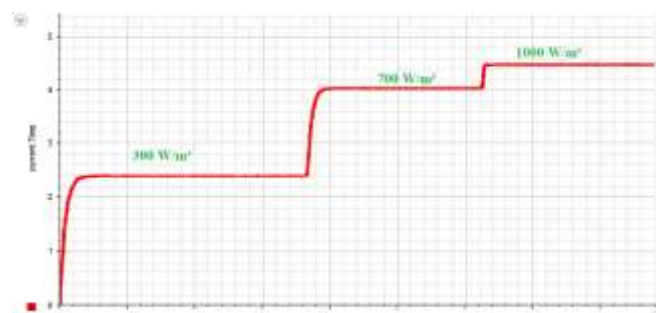


Fig. 37. The current at the output of the boost converter (Iout).

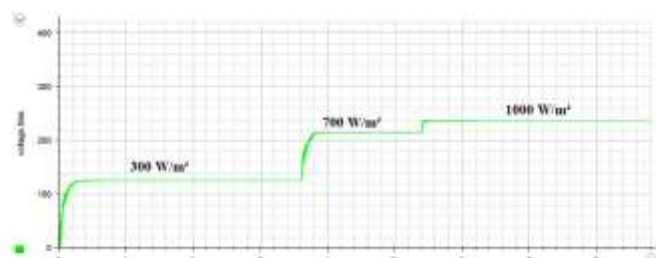


Fig. 38. the voltage at the output of the boost converter (Vout);

We find that there is no difference between the simulation and co-simulation results.

4. Conclusion

Due to a better transfer of power between the 'GPV' photovoltaic generator and the load, we performed a modeling of the entire conversion chain using Matlab. We also designed and simulated the Maximum Power Point Search Algorithm (MPPT). It forces the GPV generator to operate at its Maximum Power Point (MPP), thus inducing a total improvement in the efficiency of the electrical conversion system.

We applied the three MPPT commands chosen on the PV system by combining the PV panel, chopper, and charge. We then presented the results of the simulations for a variation of the temperature and illumination. These results show very satisfactory operation on the voltage and on the power produced, as well as on the load.

We also proposed a method to optimize a photovoltaic system based on the PSO command. The results of the simulations carried out prove the effectiveness of our approach in extracting maximum

power from photovoltaic systems compared to other commands.

References:

- [1] Castillo-Calzadilla, T., Macarulla, A. M., Kamara-Esteban, O., & Borges, C. E. (2018). Analysis and assessment of an off-grid services building through the usage of a DC photovoltaic microgrid. *Sustainable Cities and Society*, 38, 405–419.
- [2] Castillo-Calzadilla, T., Macarulla, A. M., & Borges, C. E. (2018). Design of sizing algorithms for a direct current off-grid photovoltaic installation. *IEEE Latin America Transactions*, 16(8), 2168–2176.
- [3] Roman, E., Alonso, R., Ibañez, P., Elorduizapatarietxe, S., & Goitia, D. (2006). Intelligent PV module for grid-connected PV systems. *IEEE Transactions on Industrial Electronics*, 53(4), 1066-1073.
- [4] Hua, C., & Shen, C. (1998, May). Study of maximum power tracking techniques and control of DC/DC converters for photovoltaic power systems. In *Power Electronics Specialists Conference, 1998. PESC 98 record. 29th Annual IEEE (Vol. 1, pp. 86-93)*. IEEE.
- [5] G. Notton, V. Lazarov, L. Stoyanov, Optimal sizing of a grid-connected PV system for various PV module technologies and inclinations, inverter efficiency characteristics and locations, *Renew. Energy* 35 (2010) 541–554.
- [6] V. Scarpa, S. Buso, G. Spiazzi, Low-complexity MPPT technique exploiting the PV module MPP locus characterization, *IEEE Trans. Ind. Electron.* 56 (2009)1531–1538.
- [7] Choi, J. W., Kim, Y. K., & Kim, H. G. (2006). Digital PLL control for a single-phase photovoltaic system. *IEE Proceedings-Electric Power Applications*, 153(1), 40-46.
- [8] Bennis, G., Karim, M., & Lagrioui, A. (2016). Optimization of the performance of a photovoltaic system with MPPT controller. In *Proceedings of 2015 IEEE International Conference on Renewable and Sustainable Energy, IRSEC 2015*. Institute of Electrical and Electronics Engineers Inc.
- [9] Lagrioui, A., Bennis, G., Karim, M., & Felja, M. (2018). Comparison between the conventional PSO method and the modified PSO method for the PV system under shading. *WSEAS Transactions on Systems and Control*, 13, 186–192.
- [10] Ghita, B., Mohammed, K., Ahmed, L., Nada, Z., Noureddine, S., & Ayoub, E. (2016). Optimization and modeling of a given pv system have a single phase load. *Journal of Theoretical and Applied Information Technology*, 86(1), 112–119.
- [11] Ghita, B., Mohammed, K., & Ahmed, L. (2018). Optimization of the performance of a synchronization controller for a 3-phase photovoltaic grid-connected system. *International Journal of Power Electronics and Drive Systems*, 9(2), 622–630.
- [12] Ghita, B., Mohammed, K. & Ahmed, L. (2018). Application and comparison between the conventional methods and PSO method for maximum power point extraction in photovoltaic systems under partial shading conditions. *International Journal of Power Electronics and Drive Systems*, 9(2), 631–640.
- [13] Bennis, G., Karim, M., Lagrioui, A., & Felja, M. (2018). Optimization of the performance of a synchronization controller for a 3-phase photovoltaic grid-connected system using the PSD algorithm. *WSEAS Transactions on Systems and Control*, 13, 193–200.

Contribution of Individual Authors to the Creation of a Scientific Article (Ghostwriting Policy)

The authors equally contributed in the present research, at all stages from the formulation of the problem to the final findings and solution.

Sources of Funding for Research Presented in a Scientific Article or Scientific Article Itself

No funding was received for conducting this study.

Conflict of Interest

The authors have no conflicts of interest to declare that are relevant to the content of this article.

Creative Commons Attribution License 4.0 (Attribution 4.0 International, CC BY 4.0)

This article is published under the terms of the Creative Commons Attribution License 4.0 https://creativecommons.org/licenses/by/4.0/deed.en_US